LOW-TEMPERATURE CONCENTRATION OF NICKEL IN CI-CHONDRITE PYRRHOTITE GRAINS.

E. L. Berger[1], T. J. Zega[2], and D. S. Lauretta[1]. [1]Lunar and Planetary Laboratory, University of Arizona, Tucson AZ 85721 USA (elberger@lpl.arizona.edu). [2]Naval Research Laboratory, Washington DC, 20375 USA.

Introduction: Pyrrhotite [$(Fe,Ni)_{1-x}S$] is an abundant phase in the low-temperature, aqueously altered CI chondrites. We use the crystal structure and chemistry of pyrrhotite to constrain the history of the CI chondrites.

Samples & Analytical Techniques: Samples of Orgueil (CI) were provided by the Vatican Observatory. Sulfide grains were characterized on the Cameca SX-50 electron microprobe at UA. Electron transparent thin sections were prepared and analyzed at NRL using an FEI Nova 600 FIB-SEM and a 200keV JEOL 2200FS TEM.

Results: EMPA yield an average composition, for 32 pyrrhotite grains, of: $Fe_{6.8}Ni_{0.1}S_{8.0}$ (excluding those analyses where Ni-rich and Ni-poor regions were simultaneously sampled by the beam). The metal:S ratio of these grains, 0.87, is consistent with 4C monoclinic pyrrhotite. Three grains were found to have domains with lower than average Fe:Ni ratios, and variable metal:S ratios. Compositional data for these grains is reported in Table 1.

Grain 1: The low-Ni region of this euhedral pyrrhotite grain (Fig. 1a) is compositionally consistent with 4C pyrrhotite, with a metal:S ratio of 0.87. The regions near the concentrated Ni have higher metal:S ratios, 1.02 (high-Ni) and 0.98 (low-Ni), which are inconsistent with 4C pyrrhotite. However, crystallographically, selected-area electron-diffraction (SAED) patterns taken in five orientations from high- and low-Ni regions index identically. The patterns are consistent with a twinned, single crystal of 4C monoclinic pyrrhotite [1]. Lenses of nickel-rich material are elongated along the twin boundaries (Fig. 1b).

Grain 2: This mildly altered pyrrhotite grain has areas of increased Ni that appear mottled (Fig. 1c). An EMPA spot which sampled both Ni-rich and poor regions has a composition that plots on the tie-line between monoclinic pyrrhotite and pentlandite on the Fe-Ni-S 100-135°C ternary diagram [2], suggesting a mixture of the two phases. However, TEM analyses reveal a single crystal with regions of varying Ni abundance (Fig. 1d). SAED patterns from five orientations are consistent with 4C monoclinic pyrrhotite; the geometry of the patterns does not change upon moving from Ni-rich to Ni-poor regions. The Ni-poor domain's metal:S ratio (0.88) is consistent with this crystal structure, but the Ni-rich domain's ratio (0.98) is not.

Table 1. Sulfide Compositions

Grain	Relative Ni abund.	Method	Composition (at.%)				Phase
			Fe	Ni	S	metal:S	
1	Low	EMPA	45.9	0.7	53.4	0.87	4C mPo
	Low	TEM	49.1	0.5	50.4	0.98	4C mPo?
	High	TEM	35.3	15.2	49.5	1.02	4C mPo?
2	Low	EMPA	46.1	0.6	53.2	0.88	4C mPo
	Low	TEM	46.0	0.8	53.2	0.88	4C mPo
	Mix[1]	EMPA	34.9	14.2	50.9	0.96	4C mPo?
	High	TEM	27.1	22.5	50.4	0.98	4C mPo?
3	Low	EMPA	45.4	0.9	53.7	0.86	4C mPo
	Mix[1]	TEM	51.1	1.2	47.7	1.10	4C mPo?
	High	TEM	32.1	23.3	44.6	1.24	6C mPo? Pn?

mPo = monoclinic pyrrhotite, Pn = pentlandite.
[1]Analyses overlap high and low-Ni regions

Grain 3: Unlike grains 1 and 2 which have only chemical variations, this altered grain has both chemically and structurally distinct regions (Fig. 1e-f). The compositions of the low and high-Ni domains are, within error, consistent with 4C monoclinic pyrrhotite (metal:S = 0.86) and pentlandite (metal:S = 1.24), respectively. SAED patterns from six orientations demonstrate that the low-Ni material is crystallographically consistent with its composition. Whereas, the high-Ni material, although compositionally pentlanditic, is structurally consistent with 6C monoclinic pyrrhotite [3]; SAED patterns from six orientations match this structure, although, in two orientations pentlandite is also a viable structural solution.

Discussion: 4C monoclinic pyrrhotite is in line with expected temperatures for the CI-chondrite parent body, as it is stable below ~250°C [4]. This result is consistent with temperature constraints afforded by O-isotopes (50-150°C) [5], phyllosilicate dehydration temperatures (~300°C, serpentine) [6], and the presence of cubanite (T≤210°C) [7]. However, the Ni-rich regions of grains 1 and 2 are more metal rich than expected for the 4C monoclinic structure, indicating substitution of metal atoms for vacancies. Metal:S ratios of 0.98 and 1.02 are more consistent with troilite or a more metal-rich pyrrhotite. Pyrrhotite with 16 at.% Ni has been synthesized [8], but 4C monoclinic pyrrhotite with Ni-levels equivalent to those of grains 1 and 2 have not been reported for natural samples. The Ni-rich region of grain 3 is compositionally inconsistent with pyrrhotite, and structurally inconsistent with the cubic form of pentlandite. Possible explanations include a metastable metal-rich/sulfur-poor pyrrhotite or a low-temperaure structural variant of pentlandite. Below, we briefly discuss possible scenarios for the genesis these grains.

Fluid flow through these pyrrhotite grains is an unsatisfactory mechanism for concentrating Ni. Although this scenario would be compatible with the hydrothermal history of the CI chondrites, it is difficult to reconcile this process with the localized migration of Ni, as there is no obvious pathway for its incorporation (*e.g.,* cracks, voids, veins).

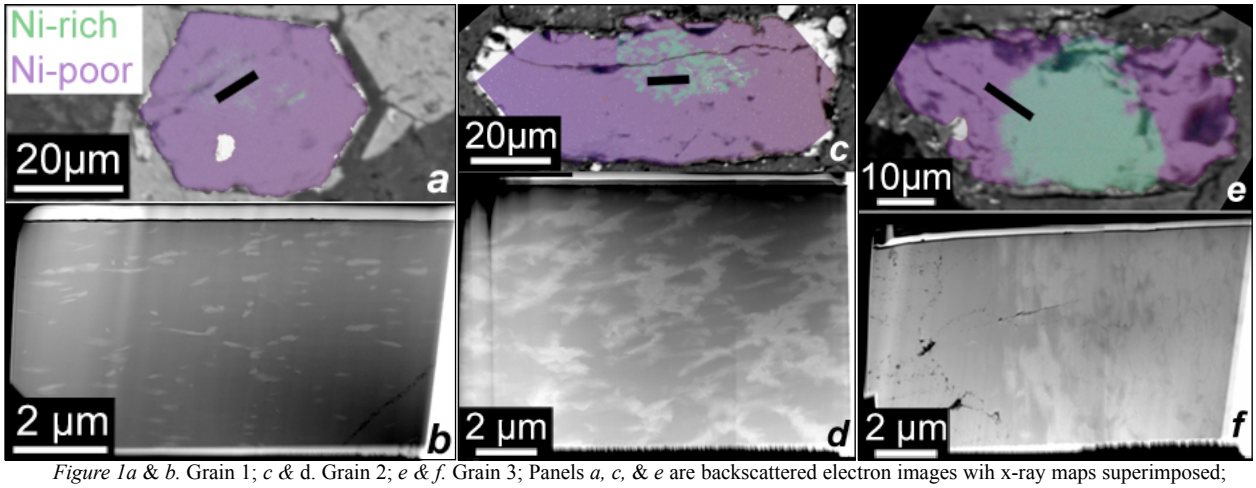

Figure 1a & b. Grain 1; *c &* d. Grain 2; *e & f.* Grain 3; Panels *a, c, & e* are backscattered electron images wih x-ray maps superimposed; Fe = red, Ni = green, S = blue. The locaton of the FIB-transect for each grain is indicated by the black rectangle. Panels *b, d & f* are high angle annular dark field images of the electron-transparent cross section prepared from each sample. High-Z material appears brighter.

Crystallization from a melt is equally unlikely, as pentlandite is an expected product. Experimental work shows that cooling from melts with $(Fe,Ni)_{1-x}S$ compositions results in mineral assemblages which include pentlandite, regardless of cooling rate [*e.g.*, 9-10].

Precipitation from a fluid could result in the textures we see, as changes in solution chemistry (pH, temperature, O- and S-fugacity) control the composition of the precipitating solids [*e.g.,* 11]. Solubility differences could dictate that Ni-rich phases precipitate first, followed closely by Ni-poor phases. However, given the 4C monoclinic crystal structure of the entirety of grains 1 and 2, a metal:S ratio of 0.875 would be expected, regardless of the Fe:Ni ratio, unless replacement of vacancies by Ni confers a free energy benefit. The low-temperature Fe-Ni-S phase relations are not well defined, nor is the low-temperature behavior of Ni in sulfides at the more basic pH values expected for the CI-chondrite parent body [12]. Experimental work is needed to explore this hypothesis.

A *solid state process* similar to the low-temperature exsolution of pentlandite from pyrrhotite is another alternative. Grain 1's Ni-lenses are similar in shape and size to both pyrrhotite-hosted exsolved submicron pentlandite seen in CM chondrites [13] and to experimentally produced pentlandite oriented along the same pyrrhotite zone axis as grain 1's lenses [10]. The failure of pentlandite to form indicates Orgueil sulfides record a different history than those of the CM chondrites. For these grains, there was enough energy in the system to concentrate Ni, but not enough to promote structural changes, *i.e.*, they are frozen-in remnants of an arrested exsolution process that failed to reach equilibrium due to sluggish kinetics and low temperatures. Metal mobility in sulfides persists at room temperature; these grains could be altered at temperatures below 100°C [8], consistent with CI-chondrite temperature constraints.

Lastly, we consider *diffusion from a fluid* due to a chemical gradient. Ni diffuses through sulfides faster than Fe, thus the migration of Ni towards the interior of a grain can result in a mottled texture [14] similar to that shown for grain 2. The differing textures amongst these three grains are due to variable starting compositions, fluid compositions, and/or duration of exposure to a fluid. Certainly, there is a trend of increased Ni-content with increased alteration of the pyrrhotite grain (1<2<3); if we assume originally euhedral habits, the bulk Fe:Ni ratios of grains 1, 2, and 3 are: ~30:1, 15:1, and 5:1, respectively. This scenario is consistent with low-temperature hydrothermal processing, but again, experimental work is needed.

Conclusion: The Ni-rich regions of these grains are incompatible with their crystal structures. The process by which they form must be consistent with the low-temperature aqueous history of the CI chondrites. Without experimental work to delineate the low-temperature phase relationships in the Fe-Ni-S system and the behavior of Ni and Fe in low-temperature solutions of varying pH, it is difficult to quantify the conditions under which the Ni migrated. We are most likely looking at (1) a snapshot of low-temperature solid state processes with enough energy to chemically, but not structurally, exsolve Ni-rich phases, or (2) low-temperature structural/compositional permutations of pentlandite and pyrrhotite.

References: [1] Tokonami M, *et al*. (1972) *Am Mineral* **57**, 1066-1080. [2] Naldrett A (1989) Magmatic Sulfide Deposits. New York: Oxford University Press, 189p. [3] DeVilliers J P R & D C Liles (2010) *Am Mineral* **95**, 148-152. [4] Wang H, *et al.* (2006) *J Sulfur Chem* **27**, 271-282. [5] Clayton R N & T K Mayeda (1999) *GCA* **63**, 2089-2104. [6] Akai J (1992) *Proc NIPR Symp Antarctic Mets* **5**, 120-135.[7] Caye R, *et al.* (1988) *Mineral Mag* **52**, 509-514. [8] Etschmann B, *et al.* (2004) *Am Mineral* **89**, 39-50. [9] Durazzo A & L A Taylor (1982) *Mineralium Deposita* **17**, 313-332. [10] Francis C A, *et al.* (1976) *Am Mineral* **61**, 913-920. [11] Barnes H L & G Kullerud (1961) *Econ Geo* **56**, 648-688. [12] Zolensky M E, *et al.* (1989) *Icarus* **78**, 411-425. [13] Brearley A and C Martinez (2010) *LPSC* **XLI**, 1689. [14] Lauretta D S, *et al.* (1998) *MAPS* **33**, 821-833.

Acknowledgements: Special thanks to the Vatican Observatory for providing samples. This work was supported by NASA grants: NNX09AC60G (DSL) and NNX08AW48H (ELB).